

Intelligent Path Tracking Hybrid Fuzzy Controller for a Unicycle-Type Differential Drive Robot

Abdullah M. Almeshal, Mohammad R. Alenezi, Muhammad Moaz

Abstract—In this paper, we discuss the performance of applying hybrid spiral dynamic bacterial chemotaxis (HSDBC) optimisation algorithm on an intelligent controller for a differential drive robot. A unicycle class of differential drive robot is utilised to serve as a basis application to evaluate the performance of the HSDBC algorithm. A hybrid fuzzy logic controller is developed and implemented for the unicycle robot to follow a predefined trajectory. Trajectories of various frictional profiles and levels were simulated to evaluate the performance of the robot at different operating conditions. Controller gains and scaling factors were optimised using HSDBC and the performance is evaluated in comparison to previously adopted optimisation algorithms. The HSDBC has proven its feasibility in achieving a faster convergence toward the optimal gains and resulted in a superior performance.

Keywords—Differential drive robot, hybrid fuzzy controller, optimization, path tracking, unicycle robot.

I. INTRODUCTION

DIFFERENTIAL drive robot are commonly used as classical robot platforms to test various control strategies due to their instable and coupled nature. We inevitably need to model the differential drive robot and understand how it steers toward the desired trajectories in order to design a proper stabilizing controller. The differential drive wheeled mobile robot has two wheels and the wheels can turn at different rates and by turning the wheels at different rates so it maneuver around turns and paths. In this study, we present a unicycle model of the differential drive robot as a basis platform to analyse the performance of the applying and optimized intelligent hybrid fuzzy logic control developed by [1].

There exist different types of controllers that were developed and adopted by various researches oncontrolling the differential drive robot. Ti-Chung Lee et al. [2] presented a solution to a tracking control problem with saturation constraint for a class of unicycle-modelled mobile robots. The authors formulated and solved using the back-stepping technique and the idea from the LaSalle's invariance principle. The proposed controller can simultaneously solve both the tracking and regulation problems of a unicycle-modelled mobile robot. Computer simulations were presented which confirmed the effectiveness of the proposed tracking control law. Practical experimental results validated the simulations.

Astudillo et al. [3] developed a tracking controller for the

dynamic model of unicycle mobile robot by integrating a kinematic controller and a torque controller based on Fuzzy Logic Theory. Computer simulations presented the performance of the tracking controller and confirmed its application to different navigation problems.

Soetanto et al. [4] bypass the problems that arise when the position of the virtual target is simply defined by the projection of the actual vehicle on that path by controlling explicitly the rate of progression of a "virtual target" to be tracked along the path. The authors have proposes a nonlinear adaptive control law that yields convergence of the (closed loop system) path following error trajectories to zero. Controller design relies on Lyapunov theory and backstepping techniques. Simulation results illustrated the performance and proved the feasibility of the control system is achieving the desired trajectories and paths.

In this paper, we discuss the performance of applying hybrid spiral dynamic bacterial chemotaxis (HSDBC) optimisation algorithm on an intelligent controller for a differential drive robot. Simulations showing the performance of the optimised controller are presented and analysed showing the superior performance of the optimisation algorithm.

II. THE UNICYCLE ROBOT MODEL

The dynamics of the unicycle type of the differential drive robot are represented as:

$$\dot{x} = v \cos \phi \quad (1)$$

$$\dot{y} = v \sin \phi \quad (2)$$

$$\dot{\phi} = \omega \quad (3)$$

where: v is the speed; ω is the angular velocity; x and y represent the position in the horizontal and vertical axes; ϕ is the heading angle (yaw angle) of the robot; v and ω are the inputs to the system. The control inputs to the system are designed in a way that by adjusting the control inputs of the linear and angular velocities, the robot converges to the desired input signals. The robot linear velocity relates to the right and left wheel velocities such that:

$$v = \frac{R}{2}(v_r + v_l) \quad (4)$$

Similarly, the robot angular velocity is expressed as:

$$\omega = \frac{R}{l}(v_r - v_l) \quad (5)$$

A. M. Almeshal, M. R. Alenezi, and M. Moaz are with the Electronics and Communication engineering department, College of technological studies, Public Authority for Applied Education and Training, P.O. Box: 23167 Safat. Code No. 13092 Kuwait (phone: +965-22314492; fax: +965-22528915; e-mail: am.almeshal@paaet.edu.kw).

Solving (4) and (5) for v_r and v_l , we get the left and right wheels linear velocities as:

$$v_r = \frac{2v + \omega L}{2R} \quad (6)$$

$$v_l = \frac{2v - \omega L}{2R} \quad (7)$$

where L is the distance between the two wheels and R is the radius of the wheels.

III. HYBRID FUZZY LOGIC CONTROL STRATEGY

The hybrid FLC controller was developed by [1] and has been proven to be efficient in controlling highly nonlinear and coupled robotic vehicle as presented in [1] and [5]-[8]. The advantage of using the hybrid FLC is that it is a model free controller that can be applied to systems with variables that are continuously changing with time. Moreover, it can be widely used in robotic vehicles with properly tuned scaling factors and gains. The hybrid FLC will be used to control the unicycle robot with proper fuzzy rules tuning and adjustments of the controller gains.

The system consists of two control loops with two hybrid FLC controllers. Each hybrid FLC controller is composed a proportional-derivative plus integral controller followed by a fuzzy controller that works together to fine tune the control signal and thus driving the robot to the desired reference path.

The fuzzy inference engine will be selected as a Mamdani-type with Gaussian membership functions that would result in smoother output values. The inputs for the hybrid FLC are the error signal, change of error and the sum of previous errors. The fuzzy membership functions are presented in Fig. 1.

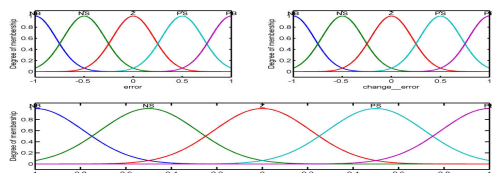


Fig. 1 Mamdani Fuzzy membership functions for the inputs and outputs of the system

The linguistic variables describing the inputs and outputs were chosen as Positive Big (PB), Positive Small (PS), Zero (Z), Negative Big (NB) and Negative Small (NS) with 25 fuzzy rule base described in Table I.

TABLE I
FUZZY RULE BASE

$e \setminus e'$	NB	NS	Z	PS	PB
NB	NB	NB	NB	NS	Z
NS	NB	NB	NS	Z	PS
Z	NB	NS	Z	PS	PB
PS	NS	Z	PS	PB	PB
PB	Z	PS	PB	PB	PB

In the next section, a hybrid spiral dynamics bacterial chemotaxis optimisation will be integrated into the control

system to find the optimal controller gains of the hybrid FLC that would minimise the overall system errors.

IV. HYBRID SPIRAL DYNAMIC BACTERIA CHEMOTAXIS OPTIMISATION ALGORITHM

The Hybrid Spiral Dynamics Bacterial Chemotaxis algorithm (HSDBC) for global optimisation was developed by [9]. The HSDBC algorithm is hybridization between the Spiral Dynamics Algorithm (SDA) developed by [10] and the Bacterial Foraging Algorithm (BFA) algorithm developed by [11]. The BFA algorithm has faster convergence speed to feasible solutions in the defined search space but has some oscillations toward the end of the search operation. The SDA algorithm has a faster computation time and a better accuracy than the BFA algorithm. Furthermore, the SDA algorithm has better stability, due to the spiral steps, when searching toward the optimum point. The HSDBC algorithm combines the strengths of BFA and SDA into a faster, stable and accurate global optimisation algorithm. This is achieved by incorporating the BFA chemotaxis part into the SDA and thus reducing the computational time and retaining the strength and performance of the SDA.

TABLE II
HSDBC ALGORITHM NOMENCLATURE

Parameter	Description
θ_{tumble}	Bacteria angular displacement on $x_i - x_j$ plane around the origin for tumbling
θ_{swim}	Bacteria angular displacement on $x_i - x_j$ plane around the origin for swimming
r_{tumble}	Spiral radius from bacteria tumble
r_{swim}	Spiral radius for bacteria swim
m	Number of search points
k_{max}	Maximum iteration number
N_{sw}	Maximum number of swim
$x_i(k)$	Bacteria position
R^n	$n \times n$ matrix

The HSDBC optimisation pseudo code is as:

Step 0: Preparation
Select the number of search points (bacteria) $m \geq 2$, parameters $0 \leq \theta_{tumble}, \theta_{swim} < 2\pi, 0 < r_{tumble}, r_{swim} < 1$ of $S_n(r, \theta)$, maximum iteration number, k_{max} and maximum number of swim, N_s for bacteria chemotaxis. Set $k = 0, s = 0$.

Step 1: Initialization
Set initial points $x_i(0) \in R^n, i = 1, 2, \dots, m$ in the feasible region at random and center x^* as $x^* = x_{i_g}(0)$,
 $i_g = \arg \min_i f(x_i(0)), i = 1, 2, \dots, m$.

Step 2: Applying bacteria chemotaxis
i. Bacteria tumble
(a) Update x_i
 $x_i(k+1) = S_n(r_{tumble}, \theta_{tumble})x_i(k) - (S_n(r_{tumble}, \theta_{swim}) - I_n)x^*$
 $i = 1, 2, \dots, m$.
ii. Bacteria swim
(a) Check number swim for bacteria i.

```

        If  $s < N_s$ , then check fitness,
        Otherwise set  $i = i + 1$ , and
    return to step (i).
        (b) Check fitness
        1. If  $f(x_i(k+1)) < f(x_i(k))$ , then
            update  $x_i$ ,
            Otherwise set  $s = N_s$ , and
    return to step (i).
        (c) Update  $x_i$ 
         $x_i(k+1) = S_n(r_{swim}, \theta_{swim})x_i(k) - (S_n(r_{swim}, \theta_{swim}) - I_n)x^*$ 
         $i = 1, 2, \dots, m$ .
    Step 3: Updating  $x^*$ 
     $x^* = x_{i_g}(k+1)$ ,
     $i_g = \arg \min_i f(x_i(k+1)), i = 1, 2, \dots, m$ .
    Step 4: Checking termination criterion
    If  $k = k_{max}$  then terminate. Otherwise set  $k = k + 1$ , and return to step 2.
    
```

The objective function is expressed in terms of the minimum mean square error of the linear and angular velocities respectively as:

$$v_{MSE} = \min \left[\frac{1}{N} \sum_{i=1}^N (v_d - v_m)^2 \right] \quad (8)$$

$$\omega_{MSE} = \min \left[\frac{1}{N} \sum_{i=1}^N (\omega_d - \omega_m)^2 \right] \quad (9)$$

Thus, the overall cost function of the system can be expressed as:

$$J = \min (v_{MSE} + \omega_{MSE}) \quad (10)$$

The HSDBC optimisation algorithm will be integrated into the system simulation files to optimise the overall mean square error of the system for both the linear and angular velocities of the robot. The HSDBC parameters were selected as described in Table III.

TABLE III
 HSDBC SIMULATION PARAMETERS

P	R	Rzw	Ns
2	0.95	0.55	2
Theta	Initial Points	Iterations	
$\pi/4$	20	100	

V. SIMULATION RESULTS

The robot was simulated to follow an eight-shaped trajectory to evaluate its performance over complex and smooth turns. The simulation was conducted using MATLAB/Simulink environment and the model was solved differentially using Runge-Kutta method. The HSDBC algorithm was integrated and simulated with 100 iterations and has successfully achieved the minimum cost function value of 0.3682 within 18 iterations approximately. Fig. 2 illustrates the convergence plot of the cost function.

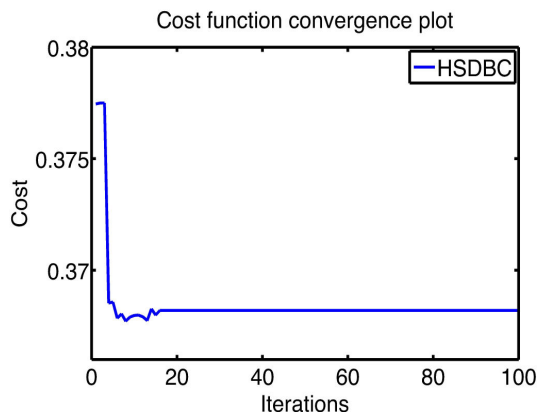


Fig. 2 Cost convergence plot

Fig. 3 presents the trajectory of the robot with heuristically tuned gains of the FLC controller. It can be seen that the robot has followed the desired path but with some oscillations that are noticeable on the path. These oscillations can be explained due to the heuristically tuned gains and more specifically the derivative gain of the hybrid FLC controller. Proper tuning of the FLC gains would certainly enhance the robot performance.

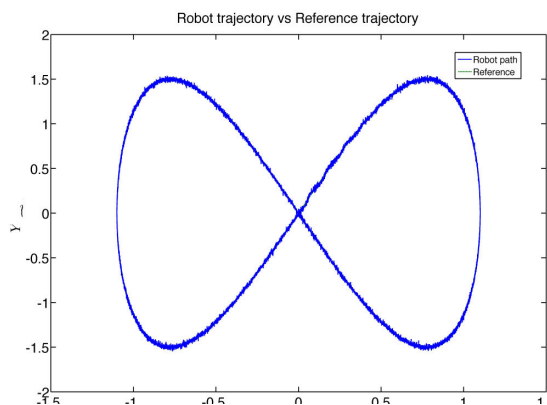


Fig. 3 The robot trajectory versus the reference trajectory with heuristically tunes gains of the FLC

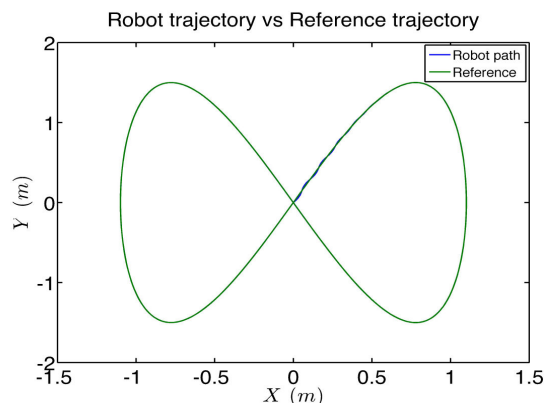


Fig. 4 Reference trajectory vs. actual robot trajectory

Fig. 4 presents the robot actual trajectory on an eight shaped reference path with the optimised hybrid FLC controller. It can be noted that the controller has been able to drive the

robot over the reference path with a high degree of accuracy as it can be noted from the error convergence of the linear and angular velocities in Fig. 5. The robot started the movement with slight oscillations and has been able to achieve a high accuracy in following the desired trajectory within 2 seconds.

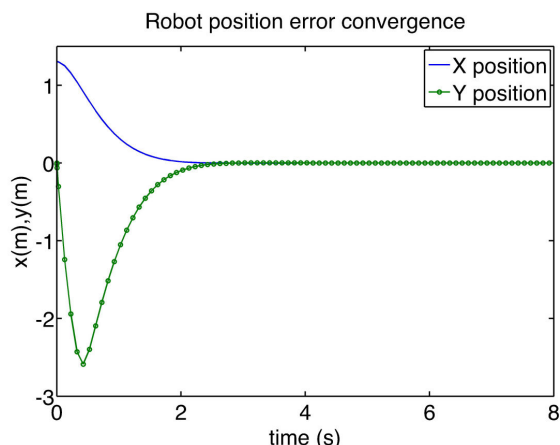


Fig. 5 Robot coordinates error convergence plot

VI. CONCLUSION

This paper presented the application of HSDBC optimisation algorithm to find the optimal performance of a hybrid FLC controller that is implemented in a unicycle robot system. The hybrid FLC performance highly depends on the proper tuning of its gains and scaling factors. The HSDBC algorithm has been proven to successfully optimise the controller within 18 iterations. The robot system was simulated and the performance of the optimised robot system was shown to be smooth and of a high degree of accuracy in following the desired trajectory. With these promising results, a future work to study the robustness of the optimised controller in counteracting uncertainties and frictions will be carried out.

REFERENCES

- [1] Almeshal, A. M., Goher, K. M., & Tokhi, M. O. (2013a). Dynamic modelling and stabilization of a new configuration of two-wheeled machines. *Robotics and Autonomous Systems*, 61(5), 443–472.
- [2] Ti-Chung Lee, Kai-Tai Song, Ching-Hung Lee, and Ching-Cheng Teng, (2001). Tracking control of unicycle-modeled mobile robots using a saturation feedback controller. *IEEE Transactions on Control Systems Technology*, 9(2), pp.305-318.
- [3] Astudillo, L., Castillo, O., L. Aguilar, A. Alanis and J. Soria, 'Intelligent Control of an Autonomous Mobile Robot using Type2 Fuzzy Logic', *Engineering Letters*, vol. 13, no. 2, pp. 565-570, 2006.
- [4] Soetanto, D., Lapiere, L., Pascoal, A., "Adaptive, non-singular path-following control of dynamic wheeled robots," *Decision and Control, 2003. Proceedings. 42nd IEEE Conference on*, vol.2, no., pp.1765,1770 Vol.2, 9-12 Dec. 2003
- [5] Almeshal, A. M., Goher, K. M., Tokhi, M. O., Sayidmarie, O., & Agouri, S. A. (2012a). Hybrid fuzzy logic control approach of a two wheeled double inverted pendulum like robotic vehicle. *Adaptive Mobile Robotics - Proceedings of the 15th International Conference on Climbing and Walking Robots and the Support Technologies for Mobile Machines, CLAWAR 2012* (pp. 681–688).
- [6] Agouri, S. A., Tokhi, O., Almeshal, A., Sayidmarie, O., & Goher, K. M. (2013). Modelling and control of two-wheeled vehicle with extendable intermediate body on an inclined surface. *Proceedings of the IASTED*

International Conference on Modelling, Identification and Control (pp. 388–393).

- [7] Almeshal, A. M., Tokhi, M. O., & Goher, K. M. (2012b). Robust hybrid fuzzy logic control of a novel two-wheeled robotic vehicle with a movable payload under various operating conditions. *Proceedings of the 2012 UKACC International Conference on Control, CONTROL 2012* (pp. 747–752).
- [8] Almeshal, A. M., Goher, K. M., Nasir, A. N. K., Tokhi, M. O., & Agouri, S. A. (2013b). Hybrid spiral dynamic bacterial chemotaxis optimisation for hybrid fuzzy logic control of a novel two wheeled robotic vehicle. *Nature-Inspired Mobile Robotics: Proceedings of the 16th International Conference on Climbing and Walking Robots and the Support Technologies for Mobile Machines, CLAWAR 2013* (pp. 179–188).
- [9] Nasir, A. N. K., Tokhi, M. O., Ghani, N. M., & Ahmad, M. A. (2012). A novel hybrid spiral dynamics bacterial chemotaxis algorithm for global optimization with application to controller design. *UKACC International Conference on Control (CONTROL 2012)* (pp. 753–758).
- [10] Tamura, K., & Yasuda, K. (2011). Primary study of spiral dynamics inspired optimization. *IEEJ Transactions on Electrical and Electronic Engineering*, 6(S1), S98–S100.
- [11] Passino, K. M. (2002). Biomimicry of bacterial foraging for distributed optimization and control. *IEEE Control Systems*, 22(3), 52–67.